PHILOSOPHICAL TRANSACTIONS OF THE ROYAL SOCIETY A MATHEMATICAL, PHYSICAL & ENGINEERING SCIENCES

A demonstrator for the SSTO launcher with combined cycle propulsion

Paul A. Czysz

Phil. Trans. R. Soc. Lond. A 1999 **357**, 2285-2316
doi: 10.1098/rsta.1999.0432

THE ROYAL SOCIETY

A demonstrator for the SSTO launcher with combined cycle propulsion

By Paul A. Czysz

Department of Aerospace and Mechanical Engineering, Parks College of Engineering and Aviation, Saint Louis University, St Louis, MO 63103, USA

Space launch systems of the 20th century are still regarded as both costly and unsafe. They have never acquired the reliability of commercial aircraft and they cannot abort from lift-off to mid-mission without massive losses. Most types of launchers are sacrificed after launch, and both hardware and environmental costs are significant. The cost of the launcher itself dominates this operation as it is the first, last and only time it flies. The user pays for the entire vehicle. For commercial aircraft operations, the frequency of flight and the lifespan of the aircraft means that the individual passenger pays about £6 for the cost of the aircraft per flight and the remainder is for fuel and operations. For commercial space launch to become both routine and economic, the need is to achieve the reliability, the sustained operation over a long lifespan, and the easy refurbishment of commercial aircraft. In seeking this solution, design studies have accepted that the ballistic missile launch may give way to either vertical or horizontal take-off aircraft using airbreathing propulsion up to a high flight Mach number and rockets thereafter. This paper examines the factors that shape the choice of airbreathing engines and airframe characteristics for SSTO space launchers, transatmospheric vehicles, boost–glide intercontinental range vehicles, and an associated demonstrator vehicle.

Keywords: space launcher; combined cycle propulsion; airbreathing propulsion; demonstration aircraft; configuration geometry; available energy analysis

1. Introduction

Over the past 15 years, propulsion has emerged once again as the enabling technology for the next generation of abortable sustained-operation vehicles. Propulsion performance purchases margin in materials, structures, systems and number of flights.

This paper looks at a path to vehicle demonstrators that can lead to future operational vehicles based on hardware performance and cost, just as aircraft did in the 1920s and 1930s, and in the 1950s, 1960s and 1970s (Augustine 1997; Forman 1997; Cook 1991). During these periods of discovery and advancement, discovery led to engineering application. Today that is not the case (IEEE/USA 1993). We must distinguish between discovery and engineering. A demonstrator is a prototype vehicle embodying the features of an operational system that gives confidence that a full-scale development can successfully proceed.

2. The need for a demonstrator

The future-generation launch vehicle must be more than reusable in order to lower the cost of access to space, as clearly shown by Penn & Lindley (1997). It must

fly to space with a usable payload and with the frequency of an airliner! As with commercial airliners, a risk and cost sharing approach provides an affordable path for all participants to acquire a new vehicle. Very high initial cost can be offset only by sustained operation and long operational life, as shown by Scott (1998). Quoting from Penn (as reported by Scott (1998)):

> Several startup companies are planning to spend about $6 billion each to develop a commercial vehicle. But they're looking at starting service with the traditional spacelift market, then to evolve the system to meet future markets (space tourism and point-to-point cargo delivery). Our analysis says you have to develop the launch system to target these non-traditional markets. If you don't design a system with a long life and robustness—[which] allows incremental flight rate increases at very low cost-per-flight—you're never going to open up those new markets.

So the demonstrator must do more than fly at high speed: it must be the basis for developing durability and confidence of operation. This is in fact a key *missing* element in most 'technology demonstrator' efforts. The key technologies relate to how effectively over a sustained period the vehicle operates, not if the vehicle operates. In fact, a demonstrator is an essential step in developing an operational vehicle, just as Mitchell's Supermarine Schneider Cup racers were the precursors to the Supermarine Spitfire.

To illustrate how the frequency of flight affects the cost the user pays, consider a large commercial cargo transport with a take-off gross weight (TOGW) of 362.8 t (800 000 lb), such as a B747 cargo. The cargo payload of 90.7 t (200 000 lb) is assumed to be sold at a price to the consumer of £2.72 kg^{-1} (£6.0 lb^{-1}). Over a 10 year period, such an aircraft would make at least 3285 flights. The gross weight is approximately the gross weight of a representative space launcher. The difference is that for a 362.8 t gross weight, the payload is less, depending on the propulsion system concept. If the airframe for a space launcher cost twice as much and the number of flights per 10 year period were consistent with the operational potential of the propulsion system, then the cost per pound to orbit for a rocket-powered launcher would be the same as for current rockets (*ca.* £4800 lb^{-1}), as shown in figure 1. If in that 10 year period the space launcher flew at the frequency of an airliner, the cost would be *ca.* £100 lb^{-1} (see figure 2). So the demonstrator needs not only to prove how it flies but how it can fly frequently.

What this does say is that reducing costs may not be a function of technology at all, but rather of utilization. The results from a number of the investigators at the Aerospace Corporation (Penn & Lindley 1997) clearly state: 'Its the flight rate!' The flight rates used to reduce the cost to the £100 lb^{-1} level are of the order of a regional commercial carrier. It is an interesting result that sets the challenge for any launcher/hypersonic aircraft demonstrator.

3. How fast is fast enough?

In Czysz (1994) the author discussed the factors that prevent the realization of a long-held desire to have ready access to space. In the present paper, the focus is a demonstrator that can provide the experimental research necessary to enable a potential operational system to be developed. Although Mach 12 is widely accepted

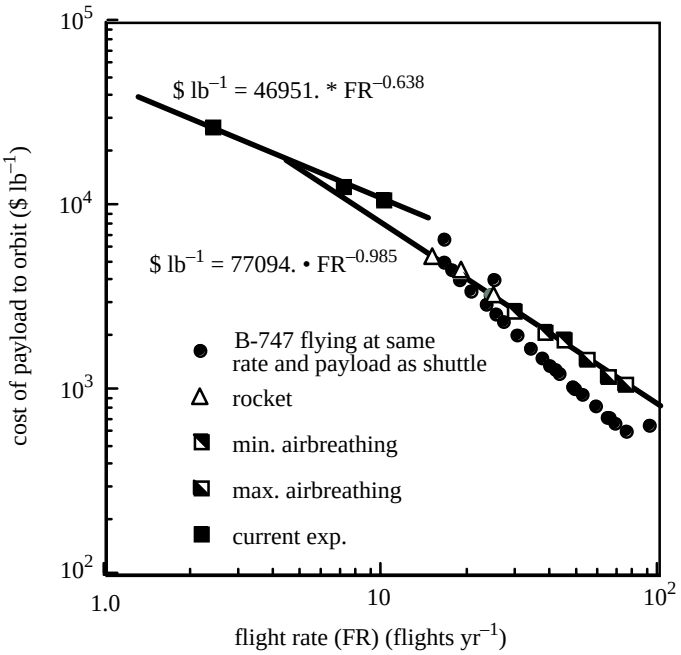

Figure 1. Flight rate, not propulsion configuration sets payload costs, circa 1985.

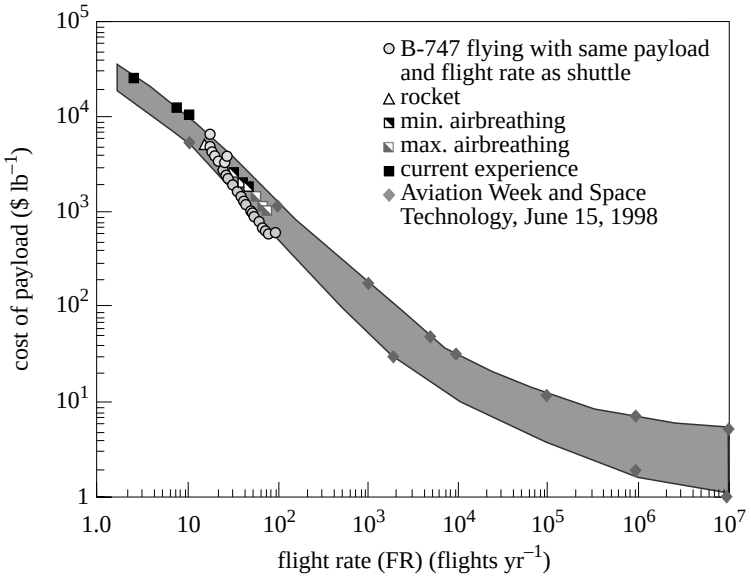

Figure 2. Flight rate sets the cost of payload to orbit, circa 1998 (Aerospace Corporation).

as the maximum airbreather speed, it is necessary to check that it is a realistic maximum airbreathing speed and a requisite demonstrator speed for a potential operational vehicle.

Three criteria are examined: the weight of the vehicle along a trajectory to orbit; the incremental vehicle propellant volume per unit change in speed; and the forebody

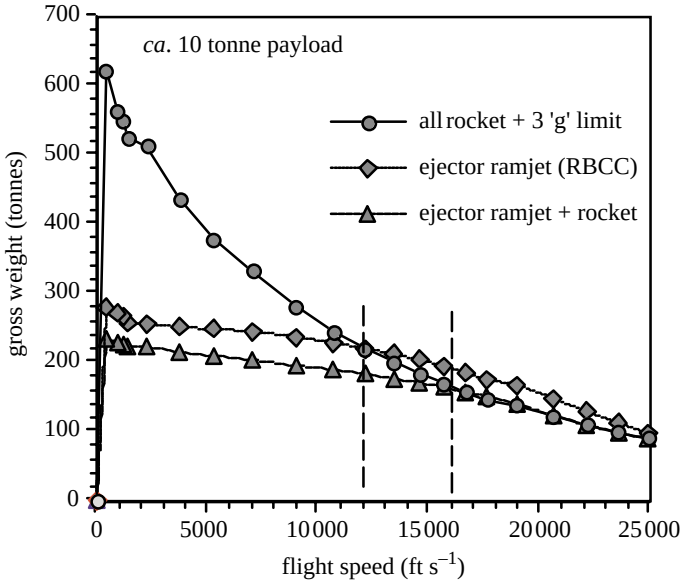

Figure 3. System weight along an ascent trajectory.

compression wall temperature. Figure 3 presents the vehicle weight along a trajectory to orbit for a system limited to a longitudinal acceleration of $3g$. In terms of the total mass to orbit, there is little difference between the three systems, although the rocket plus ramjet is slightly heavier. There is little advantage to the airbreather above the speeds indicated by the two dashed vertical lines at 12 000 and 16 000 ft s^{-1}. So, for essentially the same on-orbit weight, the RBCC that has an airbreathing cut-off in the 12 000–16 000 ft s^{-1} range can have a gross weight at lift-off of 220 t instead of 700 t for a 10 t payload. At least for achieving the minimum gross weight at lift-off, operating an airbreathing demonstrator to Mach 12–16 is adequate in terms of the potential operational system.

Figure 4 presents the change in propellant volume per unit change in flight speed. This presents a different picture to that of the previous figure. In spite of the low density of hydrogen, the propulsion efficiency (effective ISP) of the RBCC keeps the incremental volume low in the low-speed range. In the high-speed range, the volumetric increments are significantly higher than for the rocket. The vehicle of minimum volume, and, therefore, of minimum surface area, is obtained if the rocket ignition speed is between 9000 and 10 000 ft s^{-1}. So, for minimum volume, rocket transition speed does not overlap the minimum weight rocket transition speed. If the airbreathing speed is continued to Mach 17, then the volume of the airbreather-rocket vehicle is about equal to that of the all-rocket vehicle. The largest total volume would result if the airbreather continued to orbital speed. So the minimum-weight vehicle is airbreathing to between 12 000 and 16 000 ft s^{-1}, and the minimum-volume vehicle is airbreathing to between 9000 and 10 000 ft s^{-1}. Both of these charts indicate that airbreathing beyond 15 000 or 16 000 ft s^{-1} offers no significant advantage for an operational system.

As to the surface temperature, that on the forebody compression surface (that is the first ramp of the propulsion system) is the primary interest. If the radiation

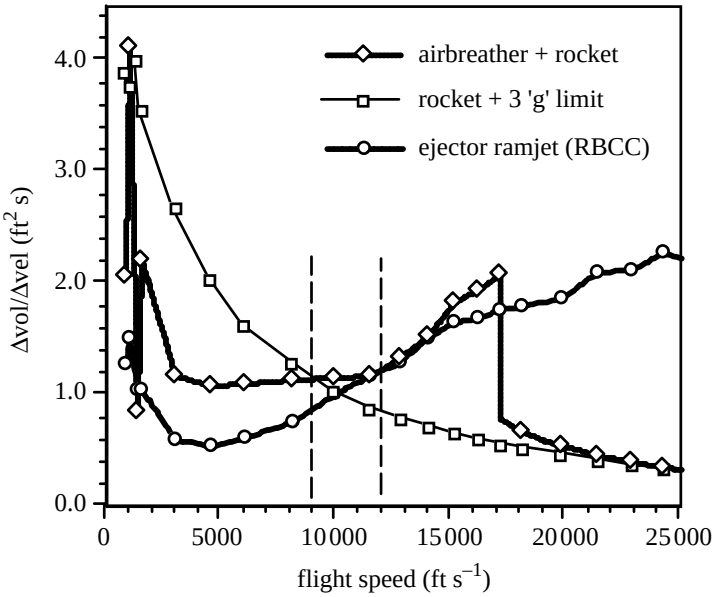

Figure 4. Change in volume per unit change in speed along an ascent trajectory.

equilibrium temperature is within the working limits of the advanced titanium thermal protection system (TPS) surface (982 °C), the weight of the forebody structure can be reduced because neither active heat removal nor heavier higher temperature materials are required. The forebody is more than just an inclined surface to the flow. It is designed to provide the correct initial compression and uniform flow into the air-breathing engine module when flying at hypersonic speeds. For airbreathing propulsion, the dynamic pressure for cruise and accelerating flight is significantly higher (up to 0.75 atm) than for high angle of attack re-entry glide vehicles (0.05 atm). As such, the acceleration and flight surface temperatures and airloads are greater than for a glider.

The equilibrium radiation surface temperature (that is the surface temperature reached when the thermal energy radiated to space equals the aerodynamic heating input) is a function of the lift loading for equilibrium flight. For a reasonable thermal–structural approach, the 982 °C level is a practical maximum for the compression side. The surface temperature of the engine module must not exceed the equilibrium radiation surface temperature, so it requires thermal management (i.e active cooling) to maintain an acceptable material temperature. The surface materials are non-structural and act as a thermal shield for the aluminium/composite load-carrying structure. The maximum Mach number for a heavier lift loading is about Mach 12 and for a lower lift loading about Mach 14.

In summary then: three criteria determine that $12\,000\ \mathrm{ft\ s^{-1}} \pm 2000\ \mathrm{ft\ s^{-1}}$ is the logical speed for transition from airbreather to rocket propulsion. This is neither an arbitrary limit nor an impractical limit to the maximum airbreathing speed. This speed range is associated with application to potentially operational systems; it is specifically not for a research vehicle designed to investigate how fast an airbreather might be able to fly (which might well involve flights to over $18\,000\ \mathrm{ft\ s^{-1}}$.)

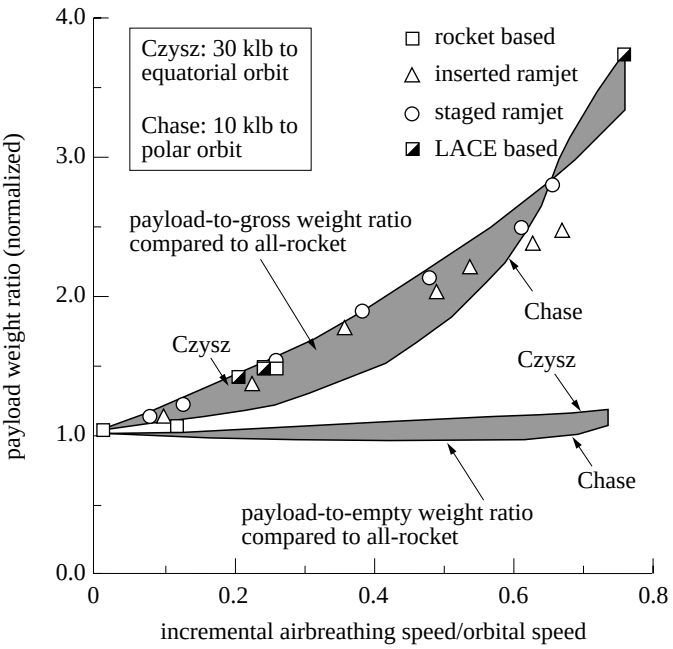

Figure 5. Payload weight ratios show empty weight ratio as constant.

4. Payload fraction

Perhaps one of the more interesting results on the subject was reported by Froning & Leingang (1990). Using the references of Chase (1990) and Nau (1967), they compared the reported results with the author's (Czysz 1991). Figure 5 shows that correlation. The important finding is that the empty-weight payload fraction is essentially constant. The apparent increase in gross-weight payload fraction is totally due to the reduction in mass ratio (i.e. reduction of the weight of carried oxidizer) with increasing maximum airbreathing speed. This is important because it means the selection of a concept can be based on sustained long-duration operating costs and assured payload survival.

Empty-weight payload fraction is the real measure of 'technology', applied industrial capability in materials and manufacturing, and in design. The gross-weight payload fraction is a measure of the propellant load carried, i.e. the mass ratio minus 1. The other observation is that the simple weight and volume sizing of Czysz (1996*a*, 1997) is not inconsistent with much more sophisticated studies.

5. Propulsion options

(*a*) *Propulsion cycles*

Eleven propulsion cycles based on hydrogen and oxygen are considered in this report. All options are integrated with a rocket motor to achieve orbital speed, for space operations, take-off, and transonic acceleration. All options have sufficient thrust potential to launch vertically and accelerate through the transonic region without excessive fuel burn, i.e. less or equal propellant to that which would be needed for

a rocket. The carried oxidizer decreases from system 1 to 10. The carried oxidizer for the KLIN cycle is equal to that for airbreathing rockets. These eleven propulsion cycles are as follows.

Rocket cycles

1. Topping cycle rocket
2. Expander cycle rocket

Rocket-derived cycles

3. Air-augmented rocket (no duct combustion)
4. Ram rocket (with duct combustion)

Deeply cooled airbreathing rocket

5. Deeply cooled rocket

Liquid air airbreathing rocket

6. LACE rocket

Deeply cooled combined cycles

7. Deeply cooled rocket + ram-scramjet
8. No. 6 plus separation and collection (ACES)

LACE-based combined cycles

9. LACE rocket + ram-scramjet
10. No. 9 with separation and collection (ACES)
11. KLIN cycle, deeply cooled turbojet plus no. 5

The descriptions of these cycles depicted in figure 6 are as follows.

Air-augmented rocket = ducted rocket = ejector rocket = secondary airflow duct with inlet driven by rocket ejector.

Ram rocket = ejector rocket where secondary airflow is used to burn additional fuel as ramjet.

Deeply cooled = an air–hydrogen heat exchanger cools secondary airflow almost to saturation. An expander turbo-compressor compresses cold gas before it is piped to an expander rocket.

LACE = liquid air cycle engine = an air–hydrogen heat exchanger cools secondary airflow to liquefaction. An expander turbopump pumps liquefied air to an expander rocket. Employing the deeply cooled or LACE rocket as an air augmented rocket or ram rocket can increase the ISP significantly.

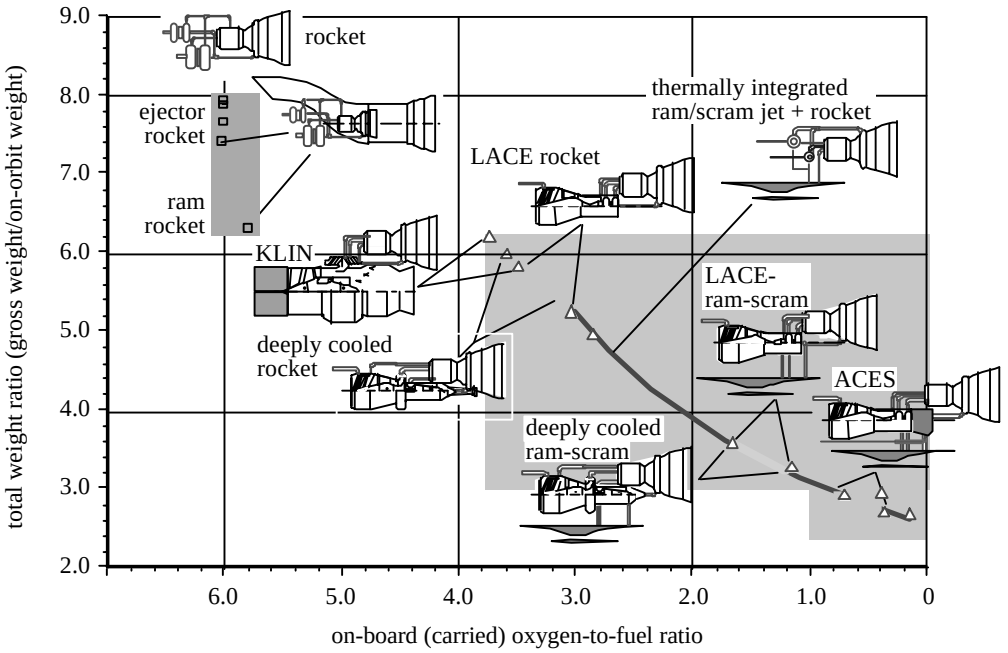

Figure 6. Air-augmented rocket propulsion provides half the benefits of fully integrated rocket-airbreathing propulsion.

Thermally integrated cycle = either a deeply cooled rocket or LACE rocket thermally integrated with ram-scramjet, i.e. all of the hydrogen flows through the heat exchanger, rocket and ram-scramjet before being burned. Deeply cooled after Rudakov & Balepin (1991). LACE after Miki *et al*. (1988).

RBCC = rocket-based combined cycle engine = thermal and physical integration of a rocket with an airbreather. Term coined by William Escher. Essentially the same as the thermally integrated cycle with emphasis on the rocket motor derivation.

ACES (1) = air collection and enrichment system = derived from a thermally integrated LACE cycle. An air-liquefying heat exchanger outputs liquid air to an expander turbopump. The turbopump outputs to a liquid-air constituent separator that outputs oxygen with a small residual of nitrogen (LEA = liquid-enriched air) and nitrogen with a small residual of oxygen (OPA = oxygen-poor air). The enriched airflows to an expander turbopump. In the collection mode, the liquid oxygen is collected for use in rocket mode and the nitrogen is ejected into an airbreathing engine to increase apparent bypass ratio.

ACES (2) = air collection and enrichment system = derived from a thermally integrated deeply cooled cycle, an air heat exchanger cooling to almost saturation upstream of an expander turbocompressor. The cold compressed gas is coupled to a gaseous air constituent separator. The oxygen with a small residual of nitrogen is sent to a liquefying heat exchanger and expander turbopump as discussed by Balepin (1996) and Balepin & Breugelmans (1997). In the collection mode, the

LEA is collected for use in rocket mode, and the OPA is ejected into an airbreathing engine to increase apparent bypass ratio.

KLIN = an air heat exchanger cooling almost to saturation upstream of a turbofan engine, resulting in constant corrected speed turbomachinery with increased airflow and negligible thermal Mach number effects. The air heat exchanger is thermally coupled to an expander rocket as discussed by Rudakov & Balepin (1991). The rocket and turbofan can be operated simultaneously.

(*b*) *Carried oxidizer*

The rocket engine itself is quite efficient, as the combustion pressure is significantly higher than that for a turbojet, but the oxidizer carried significantly increases the weight of the system. A hydrogen/oxygen rocket engine with a propellant flow ISP of 455 s has a fuel flow ISP of 3185 s! The reason for the poor propellant ISP is the oxidizer. The mass of the oxygen carried on-board can be reduced by substituting atmospheric oxygen for carried oxygen over part of the ascent trajectory (figure 6). Note that for the rocket-derived propulsion systems, combustion is always in the rocket motor. With the rocket-derived propulsion, a 32% reduction in the carried oxidizer has already been achieved. That is the oxygen-to-fuel ratio is 4.1 compared with 6.0. For the airbreathing rockets, a 43% reduction in the carried oxidizer is achieved. With the thermally integrated rocket–ram-scramjet cycles a 75% reduction in the carried oxidizer is achieved. With the ACES cycles, a 90% reduction in the carried oxidizer is possible. A rocket is still needed for operations above 160 000 ft and in space, as pointed out by Czysz and co-workers (Czysz 1995; Czysz & Murthy 1995; Czysz *et al*. 1995), so each of the propulsion configurations depicted in figure 6 is either a rocket or an airbreather system thermally and physically integrated with a rocket. The latter is very important as demonstrated by Rudakov & Balepin (1991).

The deeply cooled rocket, LACE rocket system, and KLIN cycle use atmospheric oxygen over the least speed range (to Mach 5.5 ± 0.5). What an expander cycle, deeply-cooled, KLIN cycle, and LACE achieve is to recover some of the initial energy investment as useful work, so carried energy sources can be reduced. In fact, a LACE-expander cycle can recover about one-half of the fuel liquefaction energy investment as useful work. That is not trivial. A LACE system is as much a recovery system for atmospheric air thermal energy to boil liquid hydrogen as it is a system to liquefy air! ACES further exploits the energy contained in the liquid hydrogen by permitting 90% pure atmospheric oxygen to be collected and stored in the vehicle in the outbound flight to the orbital inclination latitude. The oxygen-poor nitrogen is ejected into the ramjet engine to increase thrust without increasing fuel flow. This engine is in fact equivalent to a bypass turbojet, and is a bypass ramjet! ACES enables the vehicle to take off with either a partial or no liquid oxygen load on-board, reducing the oxygen carried on-board by half again. The weight ratio shown is the result of sizing program results from Vandenkerckhove & Czysz (1998) and from Balepin *et al*. (1995) and reflects achievable engine performance and system thrust-to-drag ratio as documented by Czysz (1996*a*).

This process is enhanced if the liquid hydrogen is converted to the para form. The para–ortho conversion is characterized by heat absorption and enhances the air-cooling process. The details are described by Balepin (1998) and Balepin *et al*.

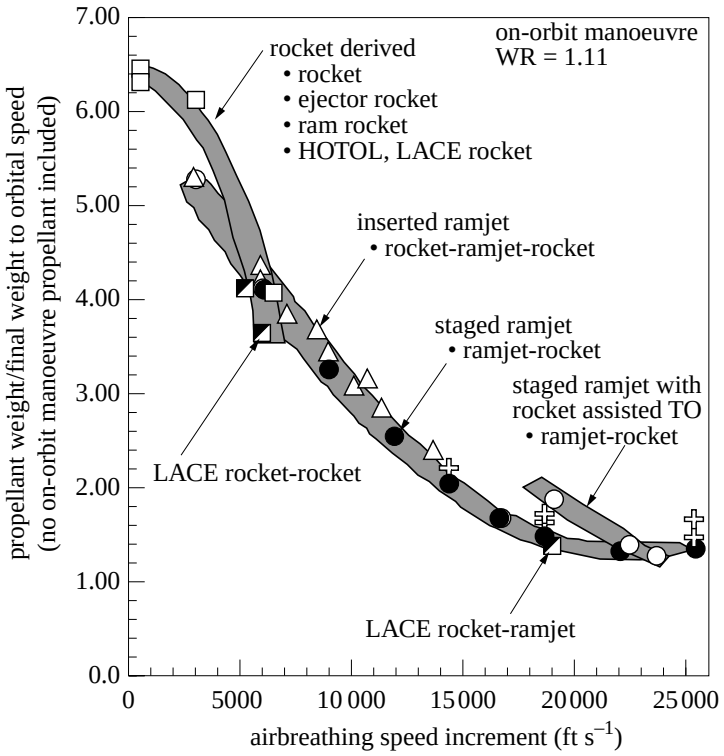

Figure 7. Airbreathing reduces the weight ratio to orbit and therefore the propellant carried.

(1994). The options are for a pressurized liquefying heat exchanger (working at several atmospheres) versus a non-pressurized liquefier. The former increases the yield in terms of liquid air generated per unit mass of liquid hydrogen. There is an ongoing discussion as to whether a liquefying cycle is necessary versus a deeply cooled cycle that takes the air nearly to saturation. In the former case, an expander cycle turbopump compresses the liquid air. In the latter case, an expander cycle turbocompressor compresses the cold gas (deeply cooled). In terms of the overall system, they can be nearly equal in performance. The actual results depend on how the individual designs are executed, not on technology.

(*c*) *Abortable launcher*

The ability to abort is a necessity for a launcher in the 21st century, and it should allow launch abort back to the launch site with the vehicle still in an operationally ready state. Where payload integrity can be preserved in an abort, and there is an on-site launch abort capability, vertical launch operations are viable for the 21st century. A LACE rocket vehicle approaches the weight ratio that is directly abortable on launch. The 'technology' required to manufacture such engines is *not* beyond current industrial capability. With a LACE rocket or KLIN cycle-powered Delta Clipper, a vertical launch rocket is launch abortable, as discussed by Czysz (1996*b*).

(*d*) *Weight ratio*

The trend of weight ratio as a function of the speed for transition from airbreather to rocket (figure 7) shows the advantage of reducing the oxidizer carried on board. Remember that whatever the propulsion configuration, it is the energy in the fuel (in this case hydrogen) that stays approximately the same. What differentiates the rocket is that it carries its own oxidizer. For commercial vehicles of long operational life it is the propellant cost that dominates, not the vehicle cost. In figure 7 the upper curve is based on rocket and rocket-derived engine cycles. Note that the HOTOL engine is a deeply cooled rocket, that is the air is not cooled beyond saturation temperature as in LACE. The lower curve is based on thermally integrated airbreathing-derived cycles. For the airbreathing transition speeds determined in § 3, the benefit in weight ratio from using an airbreather has reached 90% of its maximum.

Note that for the first and simplest step toward airbreathing, the LACE, or the deeply cooled rocket cycle, reduces the mass ratio required to reach orbit from 8 to 5 (figure 7), and the carried oxygen is nearly halved (figure 6). With an eventual ACES system, the carried oxygen might be as low as half a unit for each unit of hydrogen instead of six. So for 50 000 kg of hydrogen, the oxidizer load is 25 000 kg not 300 000 kg. That makes a significant margin for structure and payload; not to speak of a smaller lighter vehicle. That is, structural mass fraction is almost a constant fraction of the empty weight, and the empty weight is almost a constant multiple of the payload as succinctly established by Froning & Leingang (1990). So the apparent reduction in gross-weight structural fraction is indeed not due to technology but a result of the mass of oxidizer carried on-board!

(*e*) *Engine thrust-to-weight ratio*

This is always an issue with respect to airbreathing engines. Using an inlet and air thermal processing equipment could seem to offset any benefits. Rather than make contentious estimates that have doomed many US and European airbreathing and winged launcher studies, this report will take a different approach.

The question always raised concerns the empty or dry weight of the launcher, the OEW. If the engine weight were a constant, then the only changes in empty weight would be from volume and size differences. The US Space Shuttle main engine (SSME) is a high-pressure gimballed rocket engine that has an installed engine thrust-to-weight ratio ($(ET/W)_{\mathrm{i}}$) of *ca.* 65 lb thrust per lb (15.4 kg per tonne of thrust). If we select the weight of the all-rocket propulsion system as a reference, then the permissible thrust-to-weight ratio of any arbitrary engine is the required thrust divided by that reference weight. Using the sized vehicles that were derived from the weight ratio results in figure 7 gives the required installed engine thrust-to-weight ratio shown in figure 8. The step in the curve represents the change from vertical take-off to horizontal take-off. In 1966, Escher tested a supercharged ejector ramjet (SERJ) engine at flight-duplicated mass flow, temperature and pressure to Mach number 8. It generally exceeded predicted performance by 5%. The $(ET/W)_{\mathrm{i}}$ of that engine was 22 $\mathrm{lbf\,lb^{-1}}$ (45.5 $\mathrm{kg\,t^{-1}}$). So, 33 years ago a combined cycle airbreather met the requirements shown in figure 8. Is it too much to think that in 1999 this can be improved? Again the challenge is not technology, but engineering.

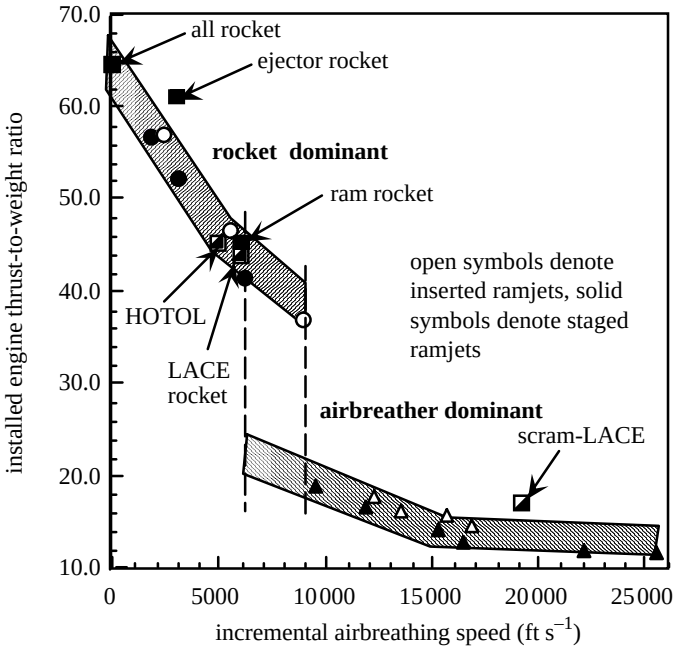

Figure 8. Installed engine thrust-to-weight ratio.

(*f*) *Wing loading*

For each propulsion concept there is a resulting gross weight and operational weight empty (OWE). With the requirement for a horizontal landing, the maximum landing wing loading is based on the OWE plus a 10% reserve for landing propellant. This sets the minimum planform area. The question is then at what weight ratio does it pay to convert to horizontal take-off. The first step towards an answer should be to examine the available design space parametrically and determine the alternatives. In order to do that, several launch modes need to be evaluated. These are vertical take-off (VTO), horizontal take-off (HTO), and air launched (AL). In all cases, the landing mode is conventional horizontal landing. The take-off (and landing) speed in knots is then

$$V_{\mathrm{TO}} = \sqrt{295.37 \frac{W/S}{\sigma C_{\mathrm{L}}}} \quad (\text{in knots } (W/S \text{ in lb ft}^{-2})). \tag{5.1}$$

Historically, clean, highly swept hypersonic configurations have a take-off lift coefficient of 0.4 at 15° angle of attack. That is, the vehicle based on a 45 lb ft^{-2} (220 kg m^{-2}) landing wing loading gives a landing speed of 108 knots (200 km h^{-1}).

The reference mode is vertical take-off and horizontal landing (VTOHL). This gives the smallest planform area and the highest lift-off vehicle thrust-to-weight ratio. In the case of an air launch or horizontal take-off mode, the take-off wing loading can size the planform area. The sizing program then has two limits. A minimum wing loading set by the landing weight (1.1 × OWE) and the maximum wing loading set by the take-off speed desired. When this is translated into gross weight (for a 7 t payload) as a function of the speed for transition from airbreather to rocket, the impact on

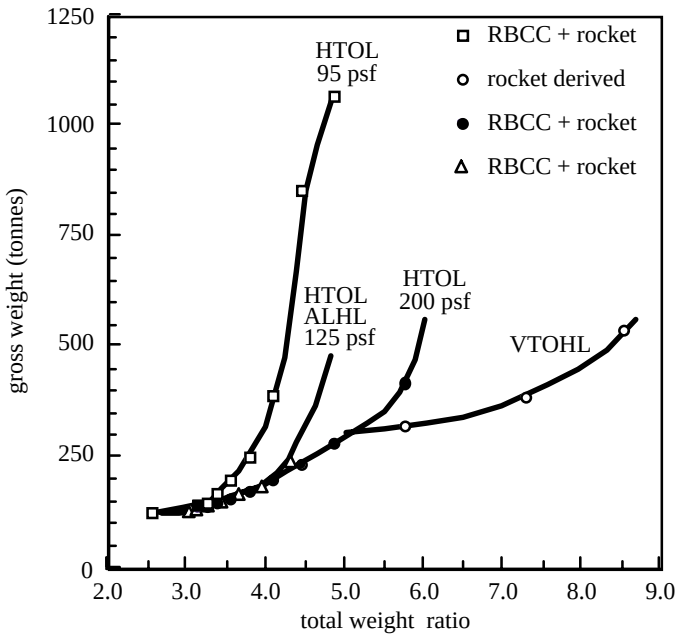

Figure 9. Wing loading drives the gross weight for a given launch mode.

weight and size is clear (figure 9). The 200 lb ft^{-2} (976 kg m^{-2}) value is a historical result that was unpublished until presented by Czysz (1993). This gives a very high take-off speed of 384 knots (711 km h^{-1}), about Mach 0.58! Vandenkerckhove used a sea-level horizontal take-off wing loading of 95 lb ft^{-2} (463 kg m^{-2}) that gives a take-off speed of 264 knots (489 km h^{-1}) in his sizing studies. For air launch (ALHL), an altitude of 27 000 ft (8.23 km) and a wing loading of 125.8 lb ft^{-2} (614 kg m^{-2}) were selected. That gives a launching speed for the carrier aircraft of Mach 0.79 (471 knots or 873 km h^{-1}). This should be well within the capability of potential carriers with current high-thrust turbofans (Trent 800 and GE CF-6/GE 90).

The high wing loading produced a divergence with the VTOHL results at a weight ratio of about 5.5. That is approximately the weight ratio for a LACE rocket. The results indicate that the higher thrust of a ram-rocket yields a lower gross weight than an ejector-ramjet for the 5500 ft s^{-1} transition point. However, the former has no potential to grow to a higher transition speed, while the latter does. With sizing for the lower take-off wing loading, the weight ratio for horizontal and vertical launch equality also falls. So, what was equivalence at a weight ratio of 5.2 for 200 lbf ft^{-2} take-off wing loading reduces to a weight ratio of about 4.1 for an air-launched vehicle with a launch wing loading of 125.8 lbf ft^{-2}, and a weight ratio of about 3.2 for a horizontal take-off vehicle with a launch wing loading of 95 lbf ft^{-2}. Referring back to figure 2 gives the transition speeds for these equivalence points as shown in table 1.

As expected, for all of the different propulsion systems, the operational empty weights (dry weight plus trapped fluids) are essentially a function of the planform area.

For the historical 200 lb ft^{-2} take-off wing loading, it was shown above that horizontal take-off (HTOL) offered an advantage for weight ratios less than 5.5. This required a gimballed rocket engine to be operating at take-off, so it could produce

Table 1. *Weight ratio and corresponding speed for transition to rocket*

weight ratio	speed
5.2	5 500 ft s^{-1}
4.1	10 000 ft s^{-1}
3.2	15 000 ft s^{-1}

nose wheel lift-off and sufficient thrust support to maintain a steep accelerating climb. The rocket was also used for transonic acceleration. With vortex flaps, the lift coefficient might be increased to 0.7, reducing the take-off speed to 290 knots (537 km h^{-1}). A more likely wing loading is that corresponding to the clean configuration take-off speed but with vortex flaps. That wing loading is 165 lb ft^{-2} (805 kg m^{-2}) and corresponds to a weight ratio of about 4.7, or a transition from airbreather to rocket of 8000 ft s^{-1}. The take-off wing loading of 95 lb ft^{-2} (463 kg m^{-2}) almost precludes horizontal take-off solutions as the transition speed from airbreather to rocket is 16 000 ft s^{-1}, or at the limit of the useful airbreathing speed for an operational system.

6. Configuration concept

(*a*) *Küchemann's* τ

The ratio of the volume to planform area was defined by Küchemann as τ:

$$\tau = V_{\text{total}}/S_{\text{p}}^{1.5}. \tag{6.1}$$

The sizing program determines maximum values of Küchemann's τ from the volume required for the systems and propellant, and from planform area sufficient for landing. When the weight ratio is inputted into the sizing program, the sizing loop balances the weight and total volume until the assumed value and the calculated values are the same. This is detailed by Vandenkerckhove & Czysz (1998).

If the wing loading is specified, then there is a single solution for τ based on the reference weight and total volume. The ratio of surface area to planform area is a function of τ and its value depends on the configuration concept geometry. The magnitude of the surface area determines the structural weight through the structural index, μ. That is:

$$\mu = W_{\text{str}}/S_{\text{wet}} \quad (\text{lb ft}^{-2}) \text{ or } (\text{kg m}^{-2}). \tag{6.2}$$

The ratio of wetted (surface) area to planform area increases as τ increases for all configuration concepts (figure 10). The region for three different classes of vehicle is indicated. For an airbreathing concept operating at $M > 6$, the geometric family has to be one of the aircraft families, i.e. *blended body, wing-body* or *waverider*, because these are designed with the underside provoking a multi-shock inlet system providing air to the engine cowl face. For these three geometric classes, with hydrogen fuel, the minimum gross weight and minimum empty weight generally occur in the vicinity of $\tau = 0.18 \pm 0.015$. Note: the waverider shown is a Nonweiler type. If the waverider is like that developed by Lewis (of the University of Maryland), the characteristics are similar to the wing-body. For a vehicle that is rocket- or airbreather-powered

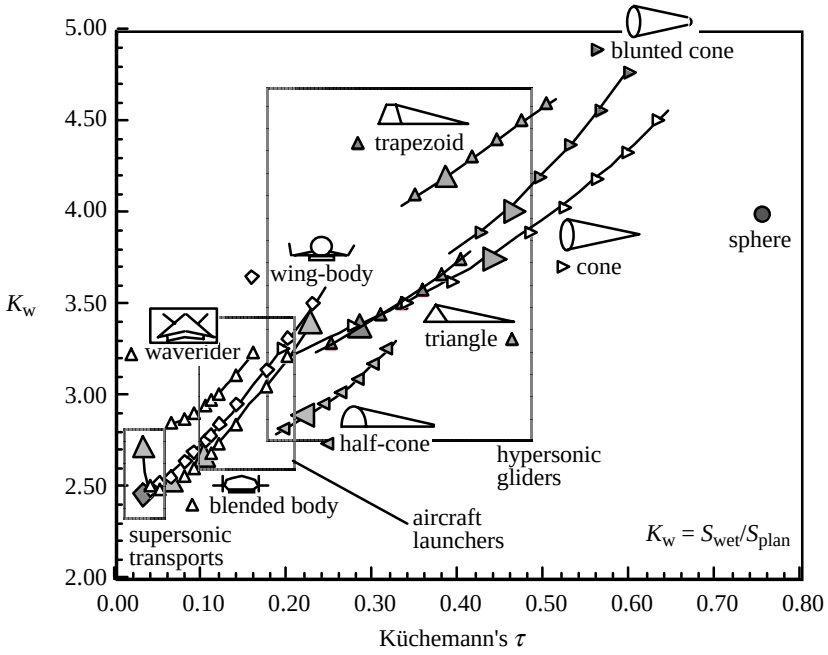

Figure 10. Surface and volume characteristics of representative hypersonic geometries.

to a Mach number not exceeding 6, then the geometric family chosen is the one yielding the least dry weight and, generally, these are the blunt based hypersonic glider configurations. Which one is the most appropriate depends on the vehicle's total volume. The most slender are the high-speed cruise aircraft that are dominated by low zero-lift drag and high lift-to-drag ratio. The open circles are results from detailed UNIGRAPHICS CAD layouts. The remainder of the points are from analytic representations of the geometry. For HTOL, the minimum-sized aircraft has too little planform area, and the planform area is increased until the take-off wing loading constraints are met. This means a τ less then the maximum, and thus a weight penalty. The implication is that unless a high transition speed is the design aim, a vertical launch vehicle will always have a smaller size and weight than a horizontal launch vehicle (as figure 9 illustrates).

The magnitude of τ for the hypersonic gliders is not without limits. As τ increases, the lift-to-drag ratio decreases, and, therefore, the glide range is affected. If a global circumference glide range is desired, then there is a limiting τ. Correlations given by Czysz & Murthy (1996*b*) that were derived by Dwight Taylor of McDonnell Douglas read as follows:

$$\left.\begin{aligned} L/D &= C_1 \exp(C_2 M), \\ C_1 &= 9.8159 - 45.934\tau + 80.466\tau^2, \\ C_2 &= -4.4148 + 4.1680\tau - 9.8272\tau^2. \end{aligned}\right\} \tag{6.3}$$

These correlations are for pointed vehicles for Mach numbers greater than 3. With a spatulate nose (Pike 1977), the lift-to-drag ratios could be up to 24% greater. Data for a number of hypersonic vehicles were correlated in that time period with respect

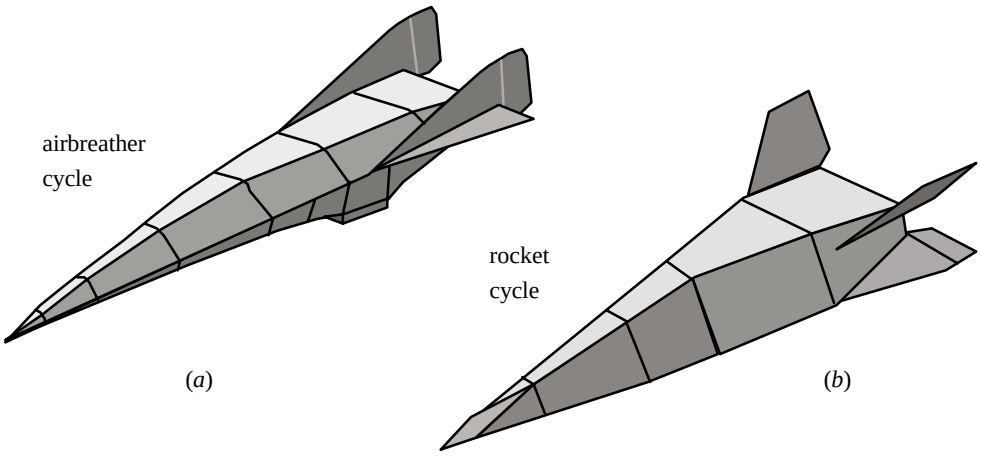

Figure 11. Hypersonic (*a*) powered aircraft and (*b*) glider.

to lateral (cross) glide range and down glide range capability as functions of lift-to-drag ratio. To achieve a global circumference down glide range capability, the cross glide range capability had to be in the 4000–4500 nautical mile range. That required a hypersonic lift-to-drag ratio of about 3. With the different MDC- and AFFDL-based hypersonic glider concepts, high Mach number lift-to-drag ratios were in the 2.7–3.5 range based on wind-tunnel data. The reason for requiring a global range glide distance is simply one of operational safety. With that capability, a vehicle in orbit can recover to its launch region (USA, Europe, Russia, China) from any orbital location from its current orbit, i.e. no waiting. To realize this capability, the region needs to span *ca.* 60° latitude. Russia spans almost twice this value, so the L/D required for a no-waiting return to Russia is about 1.9.

(*b*) *Configuration geometry*

The need is, perhaps, for a single concept that meets the research objectives required for a hypersonic flight research facility, as developed by the HYFAC team and documented by McDonnell Douglas (1970*a*). This flying research facility can accomplish the RDT & E necessary to develop a number of different potential operational vehicles as established by McDonnell Douglas (1970*b*). If the concept were a rocket-only system, or a vehicle with a low Mach number airbreathing system ($M < 6$), the concept can be based on a hypersonic glider configuration (figure 11*b*). If the concept were configured to fly at hypersonic speeds and altitudes consistent with airbreathing propulsion above Mach 6, and yet retain a high performance level as a hypersonic glider, the concept must be a hypersonic powered aircraft (figure 11*a*). If the intent is to begin with a known rocket propulsion system and then to add an airbreathing system, the glider configuration in figure 11*b* cannot be so modified. To accomplish this, the airbreathing system must be deleted from the hypersonic aircraft in such a manner that it can be incorporated at a later time, after the vehicle handling qualities and performance have been verified. Thus, the basic vehicle is rocket powered and includes the provision to mount an integrated propulsion package that can test a large variety of propulsion systems.

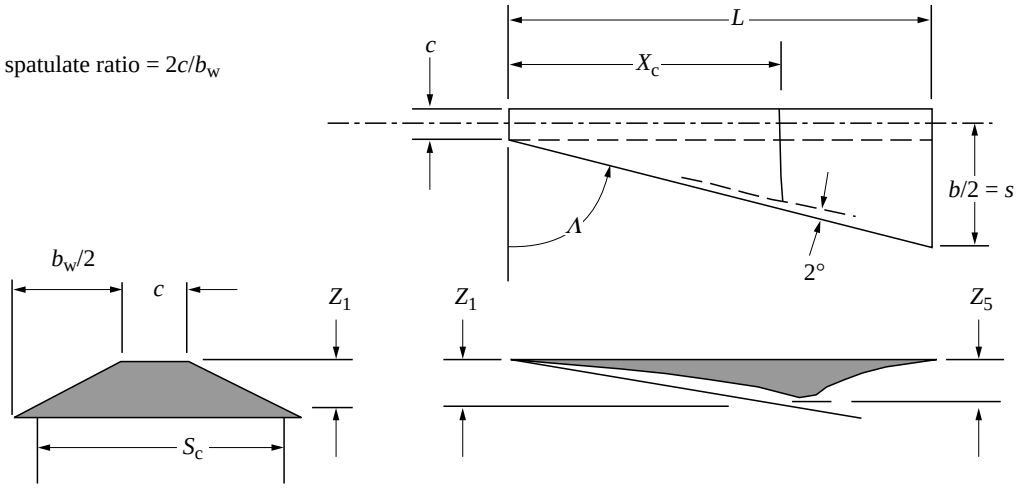

Figure 12. Spatulate, or trapezium planform configuration relationships.

(*c*) *Spatulate nose*

The geometry of the hypersonic vehicle is taken from experimental and analytical research in the UK in the mid-1960s by Pike (1972, 1977) and Townend (1966). The configurations in figure 11 can have the pointed nose replaced with a spatulate nose, as demonstrated by Pike. The spatulate nose provides a much more uniform flow to the engine face, minimizes side spill over the leading edges, and reduces forebody drag by as much as 35%. When the author visited the UK research centres in the early 1980s for the NASP project, the accomplishments of Townend, Pike, Broadbent *et al*. did not go unnoticed. As documented by Czysz (1996*b*), the spatulate nose offers additional engine sizing advantages when applying a fixed-size engine module to aircraft of differing size (see § 6 *d*).

The spatulate configuration is often given a power-law planform nose shape. The trapezoidal shape is shown in figure 12 for simplicity. The depth of the vehicle is determined by the leading-edge shock angle (ζ) when the shock is nearly shock-on-lip at the module cowl. The maximum capture area per unit planform area occurs when there is no offset from the leading edge (here shown to be 2°). For that case, and for given ζ the geometric capture area is only a function of the spatulate ratio and the axial location of the engine cowl. Equation (6.4) shows that for a reasonable maximum nose width of $(c/b) = 0.5$, the capture area per unit planform area increases by *ca.* 50%. Coupled with the zero lift drag reduction and the increased capture area, the net thrust-to-drag ratio can double. That is a principal benefit of the spatulate shape in terms of thrust-to-drag ratio:

$$\frac{A_c}{S_p} = \left(\frac{X_c}{L}\right)^2 \left[\frac{1 + \dfrac{2(c/b)}{(X_c/L)(1 - c/b)}}{1 + \dfrac{2(c/b)}{(1 - c/b)}}\right], \quad \text{where } c \geqslant 0 \text{ and } b_w \text{ is constant.} \qquad (6.4)$$

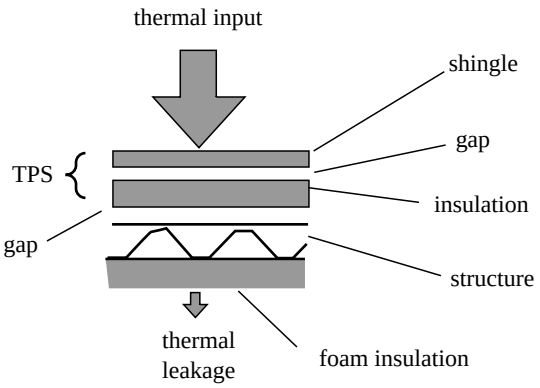

	1968–70	1983–85 est.
shingle	1.29	1.29
gap		
insulation	1.22	0.90
gap		
structure	1.45	0.74
thermal leakage		
foam insulation	0.50	0.33
	4.46	3.30 lb ft^{-2}
	21.8	16.1 kg m^{-2}

Figure 13. Structural concept for hypersonic vehicles.

(*d*) *One engine size*

There is an additional advantage of the spatulate nose. For a pointed delta planform, the length of the vehicle increases as the square root of the planform area. For an aircraft that ranges from 209 to 628 m^2, the length of the vehicle and an ejector ramjet engine module would increase from 31.4 m/2.06 m to 54.4 m/3.57 m, respectively. That would mean that for any sized aircraft within that range, a different length of engine design is required. In this era of risk abhorrence (even if it kills a successful programme) nothing could be worse than having to test every different size of engine. Using the spatulate concept, over the same size range, the length of the vehicle can be fixed, so the length of engine module can be fixed. What changes is the spatulate nose width parameter, c/b, from 0 to 0.5. Thus, one size of ejector ramjet engine can fit aircraft having many different planform areas.

As the aircraft grows larger, additional modules are added, as with any multi-engined aircraft. This means that the performance of the engine is fixed, and each engine is not an independent development. For the spatulate configuration, the engine size, thrust potential, internal drag losses, and performance are essentially constant, and one engine module size fits all. So now the tested module is the operational module and the uncertainty for one is no more or less than the other. This can be a very important consideration. If sized properly, the research demonstrator can carry the proof-of-concept engine for application to a smaller sized operational space launcher. This means a separate engine need not be qualified for flight for the initial operational space launcher.

(*e*) *Structural concept*

The structural concept (figure 13) remains appropriate and valid. This concept has withstood the test of many challenges, but remains the lowest-cost approach to high-temperature hypersonic aircraft structure. That was established by practical experience as reported by McDonnell Douglas (1970*c*). The primary structure is principally aluminium, with steel and titanium where strength is a requirement.

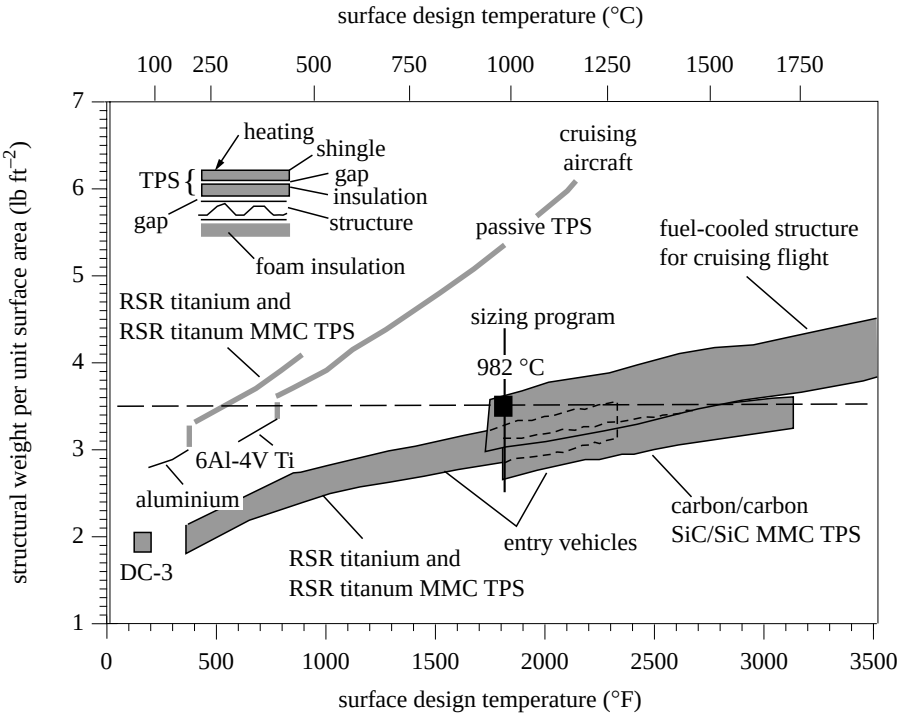

Figure 14. Representative structural specific weights for a near-term demonstrator.

The aerodynamic surface is interleaved smooth shingles with standoff and insulation material that provide a high temperature radiation surface to dissipate most of the incoming aerodynamic heating to space. Less than 3% of the incoming aerodynamic heating reaches the aluminium structure (figure 13). Table 2 shows some historical data from McDonnell Douglas (1970*a–c*) for a hypersonic research aircraft that has a 5 min test time at Mach 12 and is air launched from a C-5, much like the X-15 on the B-52. The data are circa 1968 for materials and insulation available then.

Table 3 presents the specific weight for the 1969 structural concept, an estimate and a projection of the 1983 specific weight made in 1969, and a NASA design study for a hypersonic aircraft made in 1993 from the report of Pegg *et al.* (1993), for Mach 6.0, and 1300 °F (704 °C).

The active TPS values are from a more recent source, as given by Pegg *et al.* (1993). Depending on the duration of the flight, heat can be absorbed in the airframe thermal capacitor or removed by an active thermal management system. For some short-duration (10 min or less) research flights and some orbital ascent flights, no active thermal management system is necessary. For long-duration cruise flights some means of moving the incoming thermal energy to a site at which it can be disposed of or used to perform mechanical work is required. The original concept in the 1970s was implemented using high-temperature refractory metals such as columbium (niobium), tantalum, molybdenum, and Réne 41 and other refractory alloys, which have densities greater than steel (9–17 kg m^{-3}). Today, rapid solidification rate (RSR) titanium, RSR metal matrix composites (MMC), titanium aluminide, carbon–carbon, and silicon carbide–silicon carbide composites can achieve

PHILOSOPHICAL TRANSACTIONS OF THE ROYAL SOCIETY A MATHEMATICAL, PHYSICAL & ENGINEERING SCIENCES

Table 2. *Insulated cold structure is the lightest structural system*
(To obtain kg m^{-2} from lb ft^{-2}, multiply by 4.8816.)

	thickness (in)	shingle (lb ft^{-2})	insulation (lb ft^{-2})	structure (lb ft^{-2})	tank insulation (lb ft^{-2})	tank structure (lb ft^{-2})	total (lb ft^{-2})
insulated structure, active TPS, integral tank	1.39	1.41	0.30	cold 2.0	0.33	—	4.04
insulated structure, passive TPS, integral tank	1.90	1.41	0.92	cold 2.0	0.33	—	4.66
insulated structure, passive TPS, non-integral tank	3.00	1.41	0.92	cold 2.0	0.33	—	5.20
uninsulated structure, passive TPS, non-integral tank	4.30	—	1.66	hot 4.0	0.33	0.66	6.66

Table 3. *Active and passive thermal management have approximately equal structural weights*
(To obtain kg m^{-2} from lb ft^{-2}, multiply by 4.8816.)

	thickness (in)	shingle (lb ft^{-2})	insulation (lb ft^{-2})	structure (lb ft^{-2})	tank insulation (lb ft^{-2})	tank structure (lb ft^{-2})	total (lb ft^{-2})
insulated structure, active TPS, integral tank, 1993	1.42	1.41	0.25	cold 0.84	0.33	—	2.83
insulated structure, passive TPS, integral tank, 1983	1.70	1.29	0.67	cold 0.74	0.33	—	3.03
insulated structure, passive TPS, integral tank, 1969	1.70	1.29	0.92	cold 1.45	0.33	—	3.99

the same temperature performance at much lower weight. The weight estimates based on scaling of the 1970 data are, therefore, very conservative. The concept uses conventional aircraft construction techniques for most of the aircraft, and the shingles are well within current manufacturing capabilities considering the hot isostatic pressing, superplastic forming, and diffusion bonding available in the gas turbine industry. Figure 14 is an estimate of what should be possible at the beginning of the 21st century. For longer duration flights required for long-range cruise, the advantage of active thermal management is clear. With current materials, whether actively thermally managed for cruise or passively thermally managed for exit and entry, it should be possible, in 1999 and later years, to build a structure for a hypersonic aircraft that weighs between 3.0 and 4.0 lb ft^{-2} (14.6 and 19.5 kg m^{-2}) using materials and processes available now.

7. Demonstrator aircraft

(*a*) *Demonstrator configuration*

The configuration finally recommended for the hypersonic demonstrator is an all-rocket-powered all-body configuration, with a power-law spatulate nose, that can sustain trimmed flight in excess of Mach 12 at dynamic pressures up to 1 atm (figure 15). The vehicle has been configured to be an airbreathing aircraft design, but with the second and third inlet ramps, the engine module, engine unique systems, and the initial expansion for the nozzle integrated into a removable propulsion module (figure 15*b*, *c*).†

Since there is always a caveat on developing a new aircraft and a new propulsion system simultaneously, the recommended demonstrator is then a rocket-powered vehicle that is designed to use existing rockets and to operate in a vertical take-off mode (although other take-off options can be exercised). In rocket operation, the flight controls, materials, aerodynamics and performance can be verified.

(*b*) *Demonstrator rocket motor*

The basic aircraft is all-rocket powered, carrying liquid oxygen as an oxidizer, and sub-cooled liquid hydrogen as fuel. Normal boiling point hydrogen can also be used but there is a volume penalty and the boil-off is greater. The engines are RL-10 engines as modified and already flown on the McDonnell Douglas Aerospace Delta Clipper. This is a very reliable engine and has demonstrated multiple flights and quick turnaround on the Delta Clipper programme.

(*c*) *Accommodating airbreathing modules*

The basic LOX and LH2 rocket-powered demonstrator, has been designed to incorporate airbreathing engine modules and other options. The longerons and other supporting structures have been sized to accommodate the loads associated with these

† Figure 15*b*, *c* is included for several reasons. The first is to illustrate the technical aspects of engine module installation in a demonstration vehicle of typical design. The second is to indicate the historical background to current proposals; as the quality of reproduction reveals, these drawings originally appeared in a report written 31 years ago, but their inclusion is justified for that reason alone, and they make an intriguing comparison with the Hyper-X research vehicle (which, by courtesy of NASA Langley, is shown on the flyleaf to Topic II, and is due to fly in the year 2000).

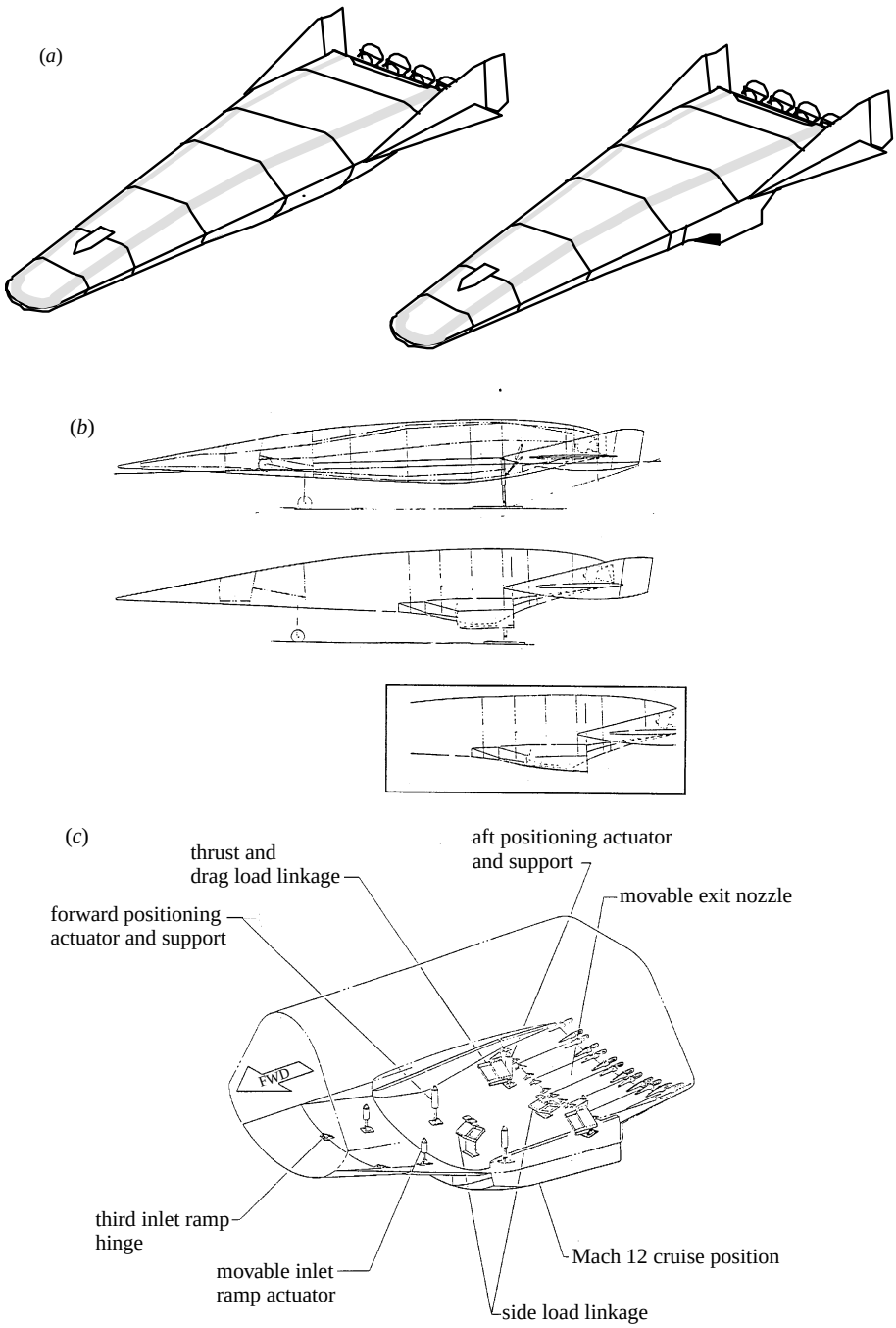

Figure 15. All rocket demonstrator with provisions for an airbreather module, and with an airbreather module installed. (*a*) Configurations; (*b*) proposed hypersonic demonstrator (1969) shown with and without the engine module installed (the inset shows the module retracted for entry and rocket operations); (*c*) engine module installation (1969).

options. It is possible, then, to incorporate a load-carrying pallet that integrates the ramps and engine modules into the rocket demonstrator airframe (as described in McDonnell Douglas (1970*b*)). The forebody of the rocket vehicle (see figure 15) forms the first compression ramp (radiation cooled) of the multiple ramp inlet, and the afterbody forms the initial expansion surface for the single expansion ramp nozzle (SERN). The ramps on the engine module must have an active thermal management system to control wall temperatures. The airbreather module is capable of translating, vertically, to change the flow path area from lower Mach numbers to the highest Mach number considered. Interchangeable modules can be designed to accommodate a number of different engine cycles, such as ram-rockets, airturboramjets, ATREX, KLIN, LACE rocket, deeply cooled ATR concept, ramjets, scramjets, and dual-mode ramjets (as shown in figure 15*b*, *c*). There will have to be a module for each propulsion system concept in most cases, although some of the ramjet/scramjet options may be adaptable in a single module. Each engine concept and its unique requirements and airflow characteristics would have to be examined and an appropriate module designed as a part of its integration, not unlike the use of different nacelles for different engines on present commercial transports. Some of these propulsion cycles have speed limitations. Engines that are limited to the Mach 5–Mach 6 regime would have to incorporate inlet cowls that can be closed, if the vehicle is not to be limited in flight speed. The focus needs to be on the vehicle size, design and a method to evaluate different propulsion systems objectively. The evaluation of the airbreathing propulsion system performance should be based on the high-speed engine/component performance assessment using available energy methods developed by Riggins of the University of Missouri, Rolla as documented by Riggins (1996), and the newly defined generalized kinetic energy efficiency parameter approach of Hoose (1996).

The installation of the ramjet module is shown in figure 15. The nose diameter and leading edges are designed for minimum practicable zero-lift drag and entropy layer thickness on the underside practicable boundary layer, and for maximum achievable lift-to-drag ratio in cruise and glide attitudes. The need to control bluntness is a requirement for satisfactory airbreather performance that has been well documented by experiments and analysis at Imperial College and Cranfield University (Bin & Harvey 1982, 1986; Edwards & Hillier 1982; Dawes & Clarke 1988). A statement of other possibilities is presented by Nonweiler (see Nonweiler's second paper in Topic I, this issue).

(*d*) *Demonstrator size*

Two methods were used to determine the demonstrator size and weight. The first used data from reports available from three decades past (Czysz 1993; Czysz *et al.* 1996*a*, *b*; McDonnell Douglas 1970*c*), scaled to current results. The second used the sizing program developed by the author in conjunction with the late Jean Vandenkerckhove (Vandenkerckhove & Czysz 1998). The converged design space for several options was investigated. There are differences between the current demonstrator configuration and the historical database because the historical database is for 1968 industrial capability. For the most part, historical studies examined both human- and computer-controlled piloting. For short-duration hypersonic research vehicles, the impact was negligible as the human-related consumables were not large compared with the electronics for the automatic flight control systems. For longer duration

space flights, the difference between human crews and automatic robotic vehicles is more significant. For this demonstrator, automatic control was chosen, based on the neural net developments that are commercially available from Accurate Automation, Inc., of Chattanooga, TN, and are already flying on the waverider LoFlyte demonstrator. The minimum size for an SSTO demonstrator (zero deployable payload) was also determined. There is a significant size and weight difference between a limited flight time hypersonic demonstrator and an SSTO demonstrator. A hypersonic demonstrator having limited flight time is not a potential SSTO launcher.

(*e*) *Definitions*

For the purpose of this study, the demonstration vehicles have no human crew and are automatically controlled. In a previous study, the hypersonic research vehicles required to provide the enabling research for six potential operational systems, four space launchers, and two hypersonic commercial transports, evolved into a requirement for a Mach 12 research aircraft that could cruise at Mach 12 for 5 min. This flight research facility was about half the cost of a comprehensive set of new ground research facilities that could accomplish about two-thirds of the research objectives achievable with the flight research facility.

Four launch approaches were evaluated, all of which were followed eventually by a conventional horizontal runway landing.

STG: staged, that is launched vertically from an expendable rocket to the Mach number and altitude required for the 5 min cruise test conditions. Glide return to base with high sink rate horizontal landing (as with the X-15).

AL: air launched from a large subsonic transport (e.g. a C5A or an An-225) with self-powered climb and acceleration to the Mach number and altitude required for the 5 min cruise test conditions. Glide return to base with high sink rate horizontal landing (as with the X-15).

HTO: horizontal take-off from a conventional airport runway and self-powered climb and acceleration to the Mach number and altitude required for the 5 min cruise test conditions. Glide return to base with high sink rate horizontal landing (as with the X-15).

VTO: vertical launch from a simple launcher/erector (such as for Military Thor or Jupiter missiles) at a launch centre, then self-powered climb and acceleration to the Mach number and altitude required for the 5 min cruise test conditions. Glide return to base with high sink rate horizontal landing (as with the X-15).

(*f*) *Sizing results*

The two roles for which vehicles were sized were a hypersonic demonstrator that could sustain a hypersonic test Mach number for 5 min, and a minimum-sized SSTO demonstrator with zero disposable payload. Weights shown in figure 16 are for each of the four launch categories based on the 1970 results. For the historical aircraft, the total structural weight divided by the total surface area is in excess of 21.77 kg m^{-2}. This is consistent with the industrial capability of 1970. However, the 1970 results used columbium (niobium), tantalum, molybdenum, Réne 41, Hastaloys and other

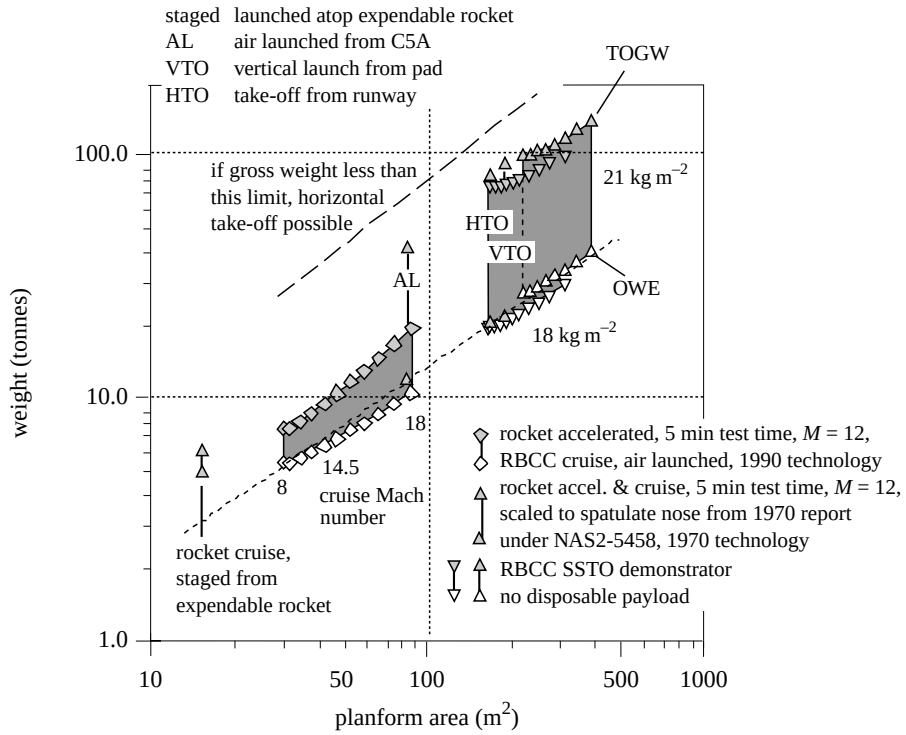

Figure 16. New sizing results for hypersonic and SSTO demonstrators.

dense materials for the external shingles. The historical vehicle results were scaled to a set of spatulate configurations with the same volume. The staged launch vehicle was too small to be considered in this process, so it remains a pointed delta configuration. These results are quite conservative. With carbon and silicon carbide ceramic and RSR titanium matrix composites, the density of current materials that can have temperatures up to 1650 °C is one-half to one-third of that for the older materials. The second set of results is for the two roles, and used the sizing program previously discussed, with the materials capability of British Petroleum in titanium MMC and of SEP Bordeaux in carbon and silicon carbide ceramic matrix materials (Czysz & Murthy 1996*a*) and with current materials within Japanese industrial capability. With current materials, the structural index should be *ca.* 18 kg m^{-2}. The vehicles were sized so that the minimum area in the ramjet engine was large enough to ensure acceptable internal losses and an acceptable net thrust.

In the AL, HTO and VTO launch approaches, vehicles are accelerated to air-breathing operating speed by rocket. This has traditionally yielded the smallest and lightest-airframe aircraft. For comparison, the air-launched concept with scramjet acceleration from $M = 6$ to $M = 12$ and then a 5 min scramjet cruise at $M = 12$ is presented. It represents the smallest and lightest research aircraft that is not launched from an expendable launcher. This vehicle was used to set the length of the demonstrator aircraft. The volume required for the other launch concepts was then accommodated by adding a spatulate width that provided that volume, as shown above. There is a clear reason for the historical study having selected the

air-launched option. C5A aircraft would have been modified as launch vehicles, and the resulting system weighed less than half the HTO and VTO launch options. The VTO option is heavier, primarily from propellant weight.

The 5 min cruise demonstrator aircraft are accelerated by combined cycle engines, following initial rocket acceleration to about Mach 3. A Mach 18 cruise vehicle with current materials would weigh about the same as the 1970s Mach 12 cruise aircraft. Note that the weight and size of the HTO and VTO demonstrators sized with the 1970 industrial capability are approaching the size of a current industrial capability SSTO demonstrator aircraft using a rocket ejector ramjet with fuel thermal management (fuel equivalence ratio in excess of one) that uses airbreathers to Mach 12.4. The SSTO demonstrator size and weight is a function of τ, which varies from 0.10 to 0.185, the latter being the left-hand boundary. So, too slender an SSTO vehicle can increase weight by over 50%.

A prior paper by Czysz & Murthy (1995) has shown that the convergence of a horizontal take-off vehicle can result in heavy penalties for horizontal take-off capability (figure 9). In figure 16, a reference line forms a practical horizontal take-off limit. None of the demonstrator configurations presented exceeds that limit.

The carrying capability of the An-225 is 100 t, and even the low-τ SSTO demonstrators are lighter than that. The air-launched option was always less costly, even when the lease cost of the launch aircraft was reflected in the estimates. The expendable launch option appears to have little value in a long-term research programme, where the frequency and number of flights is as valuable a research objective as the other objectives.

(*g*) *Demonstrator cost*

The question is now that of cost. Is it possible to extend the historical data in 1975 US dollars to the year 2000? Charles Scollatti, a former manager in Advanced Concepts at McDonnell Douglas, proposed a method of normalizing cost data for different production rates and quantities and empty weights to a fixed reference value (as given in figure 17). This eliminates the large variation in airframe cost that results from World War II (WWII) production rates compared with production rates after WWII. In fact, a P-51 would have cost about \$1 000 000 in 1975 dollars instead of the WWII reported cost. It also normalizes the changes in airframe weight and buy quantity. Such an approach appeared to provide a reasonable correlation. For comparison purposes, the Means Industrial Index was used to scale the earliest time data point (P-51, 1941) to 1986. The half-filled diamond symbols show that result. For fixed-geometry aircraft, the trends are remarkably similar. For that reason, Means Industrial Index was considered to be a reasonable basis for projecting the cost number to the year 2000 for the fixed-weight research aircraft (using scaled cost per pound) and weight addition was assessed on that basis.

Research aircraft costs were then estimated for the year 2000 based on their original weight. The cost associated with any additional weight in creating the spatulate configuration from the original pointed delta was based on an estimated year 2000 dollars per pound basis. Both the pointed delta and the spatulate configuration have the same total volume. The costs were normalized to that of the air-launched option, as that was the launch option of choice in 1970. Scaling the data over such a long period of time means that absolute values cannot be presented.

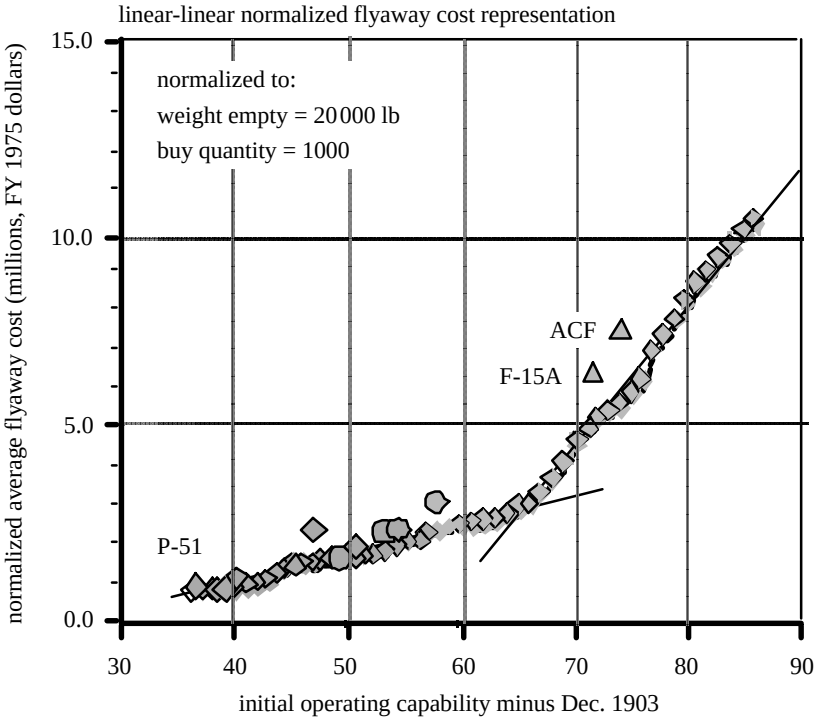

Figure 17. Correlation of normalized flyaway costs.

Total cost is based on complete research aircraft development, manufacture and a five-year flight test program based on year 2000 dollars. Even though the staged expendable research aircraft has the lowest acquisition cost, the launcher costs and the launcher's low fly rate make it the most expensive per flight by an order of magnitude. Again, it is easy to see the reason for selecting the air-launched configuration in 1970. The better option was to defer the initial cost of the scramjet, and begin with the all-rocket version that made provision for adding an airbreathing option later on. Just as before, we are suggesting the all-rocket version with the provision for an option to install an airbreather at a later date, but we do nothing that would compromise the eventual airbreather installation and performance. In this case, however, the demonstrator sized for VTO operation was chosen.

The expendable rocket-launched version may have an initial cost saving, but the cost per flight and, therefore, the cost per test point, is unacceptably high (to the point that it is a poor choice). The focus on one demonstrator, which meets most of the development requirements for a variety of space launchers and hypersonic commercial transports, provides an economical and practical path that can make maximum utilization of the international industrial capability and utilization of hardware from those who have demonstrated that it is reliable. This is a pragmatic approach to a project: wherever reliable hardware is available, use it. Do not necessarily use the technical optimum, but use one that is possible, one that is workable, and one that permits the needed experimental research to enable a future operational hypersonic vehicle.

Table 4. *Comparison of demonstrator options*

launch concept	number of flights in 5 years	RDT & E relative costs[a]	investment relative costs	operating relative costs	total relative costs	relative cost per flight
All-rocket vehicle (rocket acceleration to $M = 12$, then 5 min rocket cruise)						
staged[b]	8	0.452	0.140	1.571	0.662	14.89
air launch	180	1.000	1.000	1.000	1.000	1.000
HTO	225	1.267	1.061	1.478	1.279	1.023
VTO	180	1.319	1.333	1.265	1.309	1.308
rocket/ramjet vehicle (rocket acceleration to $M = 6$, scramjet acceleration to $M = 12$, then 5 min scramjet cruise)						
air launch	180	2.135	1.129	1.038	1.881	1.671

[a]With respect to air-launched configuration.
[b]Automatic control, uncrewed vehicle launched from expendable rocket at cruise Mach number and altitude.

8. Demonstrator conclusions

1. An all-rocket demonstrator has been identified as capable of meeting the research requirements necessary to achieve an operational space launcher or hypersonic civil transport.
2. Although the demonstrator is a rocket-powered vehicle, provisions are incorporated to accept a wide variety of airbreathing propulsion systems for testing over the entire speed range.
3. It is not necessary for the demonstrator to exceed Mach numbers of 12 to 14 in order to achieve the necessary research, as a potential operational space launcher will probably not exceed associated values of heat transfer even in re-entry.
4. Based on the fact that the weight estimates were scaled from 1970s results that used refractory metals, the results are conservative with respect to today's international industrial capabilities.
5. The cost of developing, constructing and flying a hypersonic demonstrator that can enable at least six different potential operational systems would be less than the cost of developing a single commercial airliner.
6. The all-rocket operation ensures that the critical flight regimes are not dependent solely on the performance of a research airbreathing propulsion system. A fall back system is always available.
7. The system has the option of being operated in the VTO, HTO and air-launched modes. In addition, operation as a skip-glide vehicle can produce trans-global ranges.
8. The evaluation of hypersonic propulsion systems by assessing their thrust potential provides an unambiguous determination of the parameter space that yields maximum performance, and permits comparison with other propulsion systems on a consistent basis.

This paper continues discussions about future launchers and their propulsion systems that included collaboration with four colleagues, namely H. David Froning of Flagstaff, AR, S. N. B. Murthy of Purdue University, Roger Longstaff of Essex and Leon McKinney of Saint Louis, MO, as illustrated by Czysz and co-workers (Czysz 1995, 1996*b*, 1997, 1998; Czysz & Murthy 1995; Czysz *et al*. 1995, 1997*a*, *b*).

Nomenclature

AL	Air launcher from aircraft such as C-5 or An-225
GT	Gross thrust
GW	Gross weight
I_{p}	Propulsion index $= \rho_{\mathrm{ppl}}/(\mathrm{WR}-1)$
K_{w}	$S_{\mathrm{wet}}/S_{\mathrm{pln}}$
OEW	Operational empty weight: $\mathrm{OEW} - W_{\mathrm{pay}} - W_{\mathrm{crew}}$ $W_{\mathrm{str}} + W_{\mathrm{sys}} + W_{\mathrm{prop}} + W_{\mathrm{ppl\,tnk}}$
OEW	Operational weight empty $\mathrm{GW} - W_{\mathrm{ppl}}$
P_{yo}	Empty payload fraction $= W_{\mathrm{pay/OEW}}$
P_{yg}	Gross-weight payload fraction $= W_{\mathrm{pay/GW}}$
S_{pln}	Planform area
S_{wet}	Wetted area
STG	Staged from a first rocket stage
SSTO	Single stage to orbit
TSTO	Two stages to orbit
$(T/W)_{\mathrm{eng}}$	Engine thrust-to-weight ratio $\mathrm{GT}/W_{\mathrm{prop}}$
$(T/W)_{\mathrm{to}}$	Take-off thrust-to-weight ratio GT/GW
V_{total}	Total volume $V_{\mathrm{ppl\,tnk}} + V_{\mathrm{pay}} + V_{\mathrm{sys}} + V_{\mathrm{crew}} + V_{\mathrm{void}}$
V_{ppl}	Propellant volume $V_{\mathrm{LH2}} + V_{\mathrm{LOX}}$
V_{LH2}	Liquid hydrogen volume
V_{LOX}	Liquid oxygen volume
V_{pay}	Payload volume
V_{crew}	Crew and equipment volume. $\Delta V/\Delta W_{\mathrm{ppl}}$ = change in velocity per increment propellant weight
V_{sys}	Systems volume
V_{prop}	Vehicle internal propulsion system volume
$V_{\mathrm{ppl\,tnk}}$	Propellant tanks volume
V_{void}	Unused volume
WR	Weight ratio GW/OEW
W_{ppl}	Propellant weights $W_{\mathrm{LH2}} + W_{\mathrm{LOX}}$
W_{LH2}	Liquid hydrogen weight
W_{LOX}	Liquid oxygen weight
W_{pay}	Payload weight
W_{crew}	Crew weight including crew-related equipment
W_{fluids}	Trapped fluids and consumables
W_{empty}	$\mathrm{OEW} - W_{\mathrm{fluids}}$
W_{dry}	W_{empty}
W_{str}	Structural weight
W_{sys}	Systems weight
W_{prop}	Propulsion system weight
$W_{\mathrm{ppl\,tnk}}$	Propellant tanks weight
$(W/S)_{\mathrm{to}}$	Take-off wing loading $\mathrm{GW}/S_{\mathrm{pln}}$
$(W/S)_{\mathrm{lnd}}$	Landing wing loading $1.05 \times \mathrm{OEW}/S_{\mathrm{pln}}$
RSR	Rapid solidification rate powder material, i.e. cooled from liquid in excess of $1\,000\,000\ ^{\circ}\mathrm{C\ s}^{-1}$
τ	$V_{\mathrm{total}}/(S_{\mathrm{pln}})^{1.5}$
μ_{struct}	Structural index $= W_{\mathrm{str}}/S_{\mathrm{wet}}$

References

Augustine, N. R. 1997 *Unhappy birthday: America's aerospace industry at 100*. Reston, VA: Aerospace America, AIAA.

Balepin, V. V. 1996 Air collection systems. In *Developments in high-speed-vehicle propulsion systems* (ed. S. N. B. Murthy & E. T. Curran). AIAA Progress in Aeronautics, vol. 165. Washington, DC: AIAA.

Balepin, V. V. 1998 Non-catalyst hydrogen para–ortho conversion. MSE Technology Applications White Paper, MSE Technology Applications, Inc., Butte, MT.

Balepin, V. V. & Breugelmans, F. 1997 Combined cycle for SSTO rocket: definition of the key technologies. In *Proc. XIII Int. Symp. of Air Breathing Engines*.

Balepin, V., Yoshida, M. & Kamijo, K. 1994 *Rocket based combined cycles for single stage rocket*. SAE 941166.

Balepin, V., Czysz, P., Maita, M. & Vandenkerckhove, J. 1995 Assessment of SSTO performance with in-flight LOX collection. AIAA-95-6047. In *AIAA 6th Int. Aerospace Planes Conf., Chattanooga, TN*.

Bin, L. Z. & Harvey, J. K. 1982 The experimental investigation of hypersonic turbulent boundary layer on a cold cone surface. Imperial College of Science and Technology, London, Aero Rep. 82-01.

Bin, L. Z. & Harvey, J. K. 1986 The investigation of the structure of hypersonic boundary layers on a 5° sharp cone using the electron beam fluorescence technique. Imperial College of Science and Technology, London, Aero Rep. 82-02.

Chase, R. L. 1990 Performance assessment of single-stage-to-orbit-vehicle propulsion concepts, or is atmospheric oxygen really free? AIAA 89-2293. In *AIAA 28th Aerospace Sciences Meeting, Monterey, CA*.

Cook, W. 1991 *The road to the 707*. Bellevue, WA: TYC.

Curran, E. T. 1996 Introductory paper. In *Developments in high speed vehicle propulsion systems*. AIAA Progress in Aeronautics, vol. 165. Washington, DC: AIAA.

Czysz, P. A. 1991 Hypersonic convergence. Text for hypersonic aeropropulsion design course, AE-P-450-52, Parks College of Engineering and Aviation, Saint Louis University, Saint Louis, MO.

Czysz, P. A. 1993 Rocket based combined cycle (RBCC) offers developmental and operational advantages. IAF-93-S.4.477. In *44th IAF Congress, Graz, Austria*.

Czysz, P. A. 1994 Earth to orbit aerospace planes—what prevents the realization of this long held dream? In *Int. Workshop on Aerospace Planes/Hypersonic Technology, Tokyo*.

Czysz, P. A. 1995 Interaction of propulsion performance with the available design space. In *Proc. XII Int. Symp. of Air Breathing Engines, Melbourne, Australia*.

Czysz, P. 1996*a* Propulsion concepts and technology challenges for the XXI century. In *5th Int. Symp. La Propulsion dans les Transport Spatiaux, Paris*.

Czysz, P. A. 1996*b* Energy analysis of high speed flight systems—size and thrust potential. In *JANNAF Workshop on Scramjet Performance, Albuquerque, NM*.

Czysz, P. A. 1997 Hypersonic convergence. Text for Hypersonic AeroPropulsion Design Course, AE-P-450-52, Parks College of Engineering and Aviation, Saint Louis University, Saint Louis, MO.

Czysz, P. A. 1998 Advanced propulsion concepts for the XXIst century. In *IAA Workshop on Advanced Space Propulsion Concepts, The Aerospace Corporation, El Segundo, CA*.

Czysz, P. & Murthy, S. N. B. 1995 Definition of the design space in which convergence can occur with a combined cycle propulsion system. *Acta Astronautica* **37**, 179–192.

Czysz, P. A. & Murthy, S. N. B. 1996*a* SSTO launcher demonstrator for flight test. In *AIAA 96-4574, 7th Int. Spaceplanes and Hypersonic Systems and Technology Conf., Norfolk, VA*.

Czysz, P. & Murthy, S. N. B. 1996*b* Energy management and vehicle synthesis. In *Developments in high-speed-vehicle propulsion systems* (ed. S. N. B. Murthy & E. T. Curran), vol. 165, *AIAA Progress in Aeronautics*. Washington, DC: AIAA.

Czysz, P. & Murthy, S. N. B. 1996*e* SSTO launcher demonstrator for flight test. AIAA 96-4574. In *7th AIAA Int. Spaceplanes and Hypersonic Systems and Technology Conf., Norfolk, VA*.

Czysz, P. A., Froning, H. D., McKinney, L. & Murthy, S. N. B. 1995 Payload mass and RBCC engine performance determine the industrial capability required. In *46th IAF Congress, Oslo, Norway*.

Czysz, P., Froning, H. D. & Longstaff, R. 1997*a* A concept for an international project to develop a hypersonic flight test vehicle. In *Proc. Int. Workshop on Spaceplane/RLV Technology Demonstrators, Tokyo, Japan, March 1997* and *AIAA 97-2808, 33rd Joint Propulsion Conf. and Exhibit, Seattle, WA*.

Czysz, P. A., Froning, H. D. & Longstaff, R. 1997*b* A concept for an international project to develop a hypersonic flight test vehicle. AIAA 97-7202. In *33rd IAA/AIAA/ASME/SAE/ASEE Joint Propulsion Conf., Seattle, WA*.

Dawes, A. S. & Clarke, J. F. 1988 Nonequilibrium gas flows in entropy layers. College of Aeronautics, rep. no. NFP8802, Cranfield Institute of Technology, Cranfield.

Edwards, A. J. & Hillier, R. 1982 Heat transfer and skin friction measurements in a hypersonic turbulent boundary layer at $M = 9$. Imperial College Aero rep. 82-04, Imperial College of Science and Technology, London.

Forman, B. 1997 Feeding frenzy at the trough. *Launchspace* **2**, 66.

Froning, H. D. & Leingang, J. L. 1990 Impact of aerospace advancements on capabilities of earth-to-orbit ships. In *41st Congress of the Int. Astronautical Federation, Dresden, Germany*.

Hoose, K. V. 1996 A newly defined generalized kinetic energy efficiency parameter and its application in the design of scramjet engines. In *1996 JANNAF Propulsion and Joint Subcommittee Meeting Scramjet Performance Workshop, Albuquerque, NM*.

IEEE/USA 1993 What the United States must do to realize the economic promise of space. Aerospace R&D Policy Committee, December 1993.

McDonnell Douglas 1970*a* Hypersonic research facilities studies, (HYFAC). Vol. II, part 1. Research requirements and ground facility synthesis. CR 114324, NASA Contract NAS2-5458, declassified 1982.

McDonnell Douglas 1970*b* Hypersonic research facilities studies, (HYFAC). Vol. VI. Operational systems characteristics. CR 114331, NASA Contract NAS2-5458, declassified 1982.

McDonnell Douglas 1970*c* Hypersonic research facilities studies, (HYFAC). Vols II, III and IV. CR 114323, 24, 26, 27 & 29. NASA Contract NAS2-5458, declassified 1982.

Miki, Y., Togawa, M., Tokunaga, T., Eguchi, K. & Yamanaka, T. 1988 Advanced scram-lace concept for SSTO spaceplane. IAF-88-252. In *39th Congress of the Int. Astronautical Federation, Bangalore, India*.

Nau, R. A. 1967 A comparison of fixed wing reusable booster concepts. SAE 670384. In *SAE Space Technology Conf., Palo Alto, CA*.

Pegg, R. J., Hunt, J. L., *et al*. 1993 Design of a hypersonic waverider-derived airplane. AIAA 93-0401. In *31st Aerospace Sciences Meeting, Reno, NV*.

Penn, J. P. & Lindley, A. C. 1997 Requirements and approach for a space tourism launch system. IAA-97-IAA.1.2.08. In *48th IAF Congress, Turin, Italy*.

Pike, J. 1972 The pressure on flat and anhedral delta wings with attached shock waves XXXII. *Aeronautical Quarterly* November, part 4.

Pike, J. 1977 Minimum drag bodies of given length and base using Newtonian theory. *AIAA J.* **15** (and STAR N77-15989).

Riggins, D. W. 1996 High-speed engine/component performance assessment using exergy and thrust-based methods. In *1996 JANNAF Propulsion and Joint Subcommittee Meeting Scramjet Performance Workshop, Albuquerque, NM*.

Rudakov, A. S. & Balepin, V. V. 1991 Propulsion systems with air precooling for aerospaceplane. SAE 911182. In *SAE Aerospace Atlantic, Dayton, OH.*

Scott, W. B. 1998 Airline operations offer paradigm for reducing spacelift costs. *Aviation Week and Space Technol.* **148**, 64–67.

Townend, L. H. 1966 Ramjet propulsion for hypersonic aircraft. In *Royal Aircraft Establishment, TM Aero, 917 and Euromech 3 Colloquium, Aachen, Germany, February 1966.*

Vandenkerckhove, J. & Czysz, P. 1998 Transatmospheric vehicle sizing. In *Developments in High Speed Vehicle Propulsion* (ed. E. T. Curran & S. N. B. Murthy).

PHILOSOPHICAL TRANSACTIONS OF THE ROYAL SOCIETY A MATHEMATICAL, PHYSICAL & ENGINEERING SCIENCES